Archives of Biochemistry and Biophysics 629 (2017) 8–18

Contents lists available at ScienceDirect

Archives of Biochemistry and Biophysics

journal homepage: www.elsevier.com/locate/yabbi

Histidine substitution in the most flexible fragments of firefly luciferase modifies its thermal stability

Mahdie Rahban [a], Najmeh Salehi [a], Ali Akbar Saboury [a, *], Saman Hosseinkhani [b, **], Mohammad Hossein Karimi-Jafari [a], Rohoullah Firouzi [c], Nasrollah Rezaei-Ghaleh [d], Ali Akbar Moosavi-Movahedi [a]

[a] Institute of Biochemistry and Biophysics, University of Tehran, Tehran, Iran
[b] Department of Biochemistry, Faculty of Biological Sciences, Tarbiat Modares University, Tehran, Iran
[c] Department of Physical Chemistry, Chemistry and Chemical Engineering Research Center of Iran, Tehran, Iran
[d] Max Planck Institute for Biophysical Chemistry, Goettingen, Germany

ARTICLE INFO

Article history:
Received 31 May 2017
Received in revised form
8 July 2017
Accepted 11 July 2017
Available online 12 July 2017

Keywords:
Thermostability
Flexibility
Rigidity
Protein dynamics
Psychrophilic enzyme

ABSTRACT

Molecular dynamics (MD) at two temperatures of 300 and 340 K identified two histidine residues, His461 and His489, in the most flexible regions of firefly luciferase, a light emitting enzyme. We therefore designed four protein mutants H461D, H489K, H489D and H489M to investigate their enzyme kinetic and thermodynamic stability changes. Substitution of His461 by aspartate (H461D) decreased ATP binding affinity, reduced the melting temperature of protein by around 25 °C and shifted its optimum temperature of activity to 10 °C. In line with the common feature of psychrophilic enzymes, the MD data showed that the overall flexibility of H461D was relatively high at low temperature, probably due to a decrease in the number of salt bridges around the mutation site. On the other hand, substitution of His489 by aspartate (H489D) introduced a new salt bridge between the C-terminal and N-terminal domains and increased protein rigidity but only slightly improved its thermal stability. Similar changes were observed for H489K and, to a lesser degree, H489M mutations. Based on our results we conclude that the MD simulation-based rational substitution of histidines by salt-bridge forming residues can modulate conformational dynamics in luciferase and shift its optimal temperature activity.

1. Introduction

Firefly luciferase is a monomeric protein (62 kD) composed of two globular domains [1,2]. The crystal structures of firefly luciferase from *Photinus pyralis* and *Lampyris turkestanicus* show a large N-terminal domain (residues 1–436), a flexible hinge (437–439) and a small C-terminal domain (residues 440–550) [3,4]. There is a wide cleft between the two domains containing many conserved residues in their surfaces [5]. Light emission of luciferase is used in a wide variety of biochemical assays in clinical, industrial and scientific research applications [6,7]. However, several factors limit further application and development of this technology, one of them is the low stability of luciferase enzyme in the room and human physiological temperature [8–12].

Thermal stability is an important factor in medical and industrial applications of proteins. Thermal stability of proteins is affected by various factors, including packing density in the hydrophobic core, number of disulfide bonds, strength of electrostatic interactions, length and anchoring of surface loops, stabilization of helices, conformational rigidity and local structural entropy [13–16]. Several approaches have been developed for engineering thermally stable proteins. One approach is rational structure-based design, by which protein structure and molecular modeling data combined with biochemical data are evaluated in order to propose a number of candidate mutations for improving protein stability at higher temperature. These mutations are selected based on their expected capacity to enhance Van der Waals interactions, hydrogen bonds, salt and disulfide bridges, among others [17–20].

In site-directed mutagenesis, selection of mutation sites is the most crucial step [21]. Systematic studies of protein sequences of thermophilic proteins show higher occurrence of hydrophobic and charged residues but lower frequency of polar residues [22]. The

* Corresponding author.
** Corresponding author.
E-mail addresses: saboury@ut.ac.ir (A.A. Saboury), saman_h@modares.ac.ir (S. Hosseinkhani).

http://dx.doi.org/10.1016/j.abb.2017.07.003
0003-9861/

average proportion of charged residues is also higher at the surface of thermophilic proteins [23]. Polar amino acids prefer to be surrounded by water, but when they are buried within the protein, they usually participate in hydrogen bonds with other side chains or the protein main chain [24]. In addition, studies on thermophilic protein genomes showed the content of the histidine residue to be significantly lower and the proportion of charged amino acid (Lys, Arg, Asp, Glu) higher [22,25]. Several studies have further revealed that the flexible regions of enzymes are the early targets of protein unfolding [26]. In general, flexible residues which have fewer contacts with other amino acids are more likely to produce local disorder inside the highly connected network of non-covalent interactions within proteins [27,28]. As a result, a common strategy to improve thermal stability of mesophilic proteins is to introduce new salt bridges or increase the number of hydrogen bonds, particularly in the solvent exposed flexible region of proteins [29–32]. Nevertheless, it is usually difficult to predict which region in a protein is most suitable for this strategy [33–35].

In the present work, MD simulations were carried out to explore the key factors governing the thermal stability of firefly luciferase. Consequently, these results are utilized for design of proper mutants that may be used in medical and industrial applications. Firefly luciferase has 14 histidine residues, two of them located in the C- terminal domain [3]. By calculating the root mean square fluctuation (RMSF) of backbone atoms at two temperatures (300 and 340 K) thermal sensitive (flexible) regions of luciferase were identified. Histidine461 and histidine489 are located in the flexible regions, therefore we decided to substitute them with a negatively charged residue, aspartate, or a positively charged residue, lysine, to evaluate whether the altered salt bridge and hydrogen bonding propensities of these regions improve protein thermal stability. Our results show that histidine substitution by charged residues modifies conformational flexibility in luciferase and alters its temperature stability.

2. Materials and methods

2.1. Materials

The following materials were obtained from the indicated sources: Isopropyl-D-thiogalactopyranoside (IPTG), ATP (Roche); D-luciferin potassium salt (Resem); ANS, 8-anilino-aphthalene-1-sulfonic acid (Merck, Germany); PrimeSTAR HS DNA polymerase and DpnI were purchased from Takara (Japan), plasmid extraction kit, gel purification kit, PCR purification (Bioneer CO. South Korea), Ni-NTA spin kit (QIAGEN Inc.).

2.2. Methods

2.2.1. Site-directed mutagenesis

For the construction of the single mutants, including H461D, H489K, H489D and H489M, site-directed mutagenesis was performed using the Quick-change PCR. The desired point mutants for interesting position was generated by site-directed mutagenesis on pET16b-luc using the following mutagenesis primers (underline letters represent the mutant codons):

H461D: 5′ … GATATTGTTACAAGACCCCAACATCTTCGACG … 3′
H489K: 5′ … GTTGTTGTTTTGGAGAAAGGAAAGACGATGAC … 3′
H489D: 5′ … GTTGTTGTTTTGGAGGACGGAAAGACGATGAC … 3′
H489M: 5′ … GTTGTTGTTTTGGAGATGGGAAAGACGATGAC … 3′

PCR was carried out using Pfu DNA polymerase under the following conditions: initial denaturation at 95 °C for 1 min, 18 cycles (95 °C for 1 min, 55 °C for 1 min and 68 °C for 11 min), and a final extension for 10 min at 68 °C. PCR products were treated with Dpn I (37 °C, overnight) restriction endonuclease to eliminate the methylated DNA templates. Subsequently, the mutagenesis products were purified using a cleanup kit to remove redundant primers. Thereafter, DH5α competent cells were used as cloning hosts for the transformation of the nicked vector DNA containing the desired mutations. The amplified plasmids were extracted from cultured DH5α cells by using of plasmid extraction kit. In order to confirm the correct mutation, the plasmids were sequenced by an automatic sequencer (Macrogen Corp.), using T7 promoter universal primer. Then, the stock DH5α cells, which harboring mutated plasmid were cultured overnight at 37 °C in 10 ml LB. The plasmids were extracted and transformed to BL21 cells by the heat shock method [19,36].

2.2.2. Protein expression and purification

Ten milliliters of LB medium containing 50 μg/ml ampicillin with a fresh bacterial colony harboring the expression plasmid were inoculated and grown at 37 °C overnight. Then 200 ml of medium with 500 μl overnight cultures was inoculated and grown at 37 °C with vigorous shaking until the OD_{600} reached 0.6–0.9 at 600 nm (A_{600}). Then, IPTG and lactose were added to the solution to final concentrations of 1 mM and 4 mM, respectively, and the mixture incubated at 18 °C overnight with vigorous shaking. The cells were harvested by centrifugation at 5000*g* for 15 min. The cell pellet was resuspended in lysis buffer (50 mM Tris-HCl, 300 mM NaCl, 10 mM imidazole (pH 7.8)). Purification of His_6-tagged fusion protein was performed with the Ni-NTA spin column as described by the manufacturer (QIAGEN). The purity of luciferases was verified by SDS-PAGE analysis [36].

2.2.3. Characterization of kinetic parameters

K_m value for ATP was determined by assaying 5 μl of diluted enzyme in 25 μl of assay reagent, in the addition of 20 μl of the various concentrations of ATP (from 0.004 to 8 mM). The estimation of luciferin (LH_2) kinetic constants was performed in a similar way, except that in addition of the various concentrations of luciferin (from 0.01 to 2.5 mM) were used. Approximate protein concentrations were calculated using a Bradford assay, and relative specific activities (enzyme activity vs protein concentration) were also calculated. To obtain the optimal temperature of activity for native and mutant luciferases, activities were measured in the range of 5–45 °C. Moreover, the optimum pH of activity of both enzymes was measured by incubation of enzyme in a mixed buffer in the pH range of 5–11. Bioluminescence emission spectra of purified enzymes were obtained using Cary-Eclipse luminescence spectrophotometer (Varian) from 400 to 700 nm wavelengths. Reactions were initiated by the addition of 300 μl of 50 mM Tris–HCl buffer (pH 7.8), including 2 mM ATP, 5 mM $MgSO_4$, and 1 mM luciferin, to 100 μl of a purified luciferase solution in a quartz cell [19]. All experiments are repeated at least 3 times.

2.2.4. Thermal inactivation and thermal stability studies

To study thermal inactivation, the purified luciferases (10 μg/ml) were incubated in the range of 20–50 °C for 5 min. Enzyme activities were measured at room temperature (25 °C), and the remaining activity was recorded as a percentage of the original activity after incubation for 2 min on ice. Thermal Stability rates of the luciferases were studied by incubating enzyme solutions (10 μg/ml of enzyme in 50 mM Tris-HCl pH 7.8) in a circulating water bath at 35, 30 and 25 °C for 0–45 min. At regular intervals of 0–45 min, samples were removed and cooled on ice (2 min), and the remaining activity was determined. The activity of the enzyme solution kept on ice was considered as the control (100%) [19]. The data were fitted to first-order plots and analyzed, with the first-

order rate constant measured (k_d) by a linear regression of ln (remaining activity) versus the incubation time (t). Half-lives of the luciferase variants were calculated by the equation, $t_{1/2} = \ln 2/k_d$. All experiments were carried out by three technical replicates.

2.2.5. Structural analysis

To obtain a more accurate result, purified luciferase was used in structural analysis, including extrinsic and intrinsic fluorescence studies. The purified luciferase samples were dialyzed in a dialysis buffer containing 50 mM Tris–HCl, 1% glycerol, 1 mM EDTA, 150 mM NaCl, 2 mM β-mercaptoethanol, and 0.8 mM ammonium sulfate (pH 7.8) at 4 °C [36]. Fluorescence studies were carried out on a Cary-Eclipse luminescence spectrophotometer (Varian) at 25 °C. Intrinsic fluorescence was determined using 0.02 mg/ml enzymes. The emission spectra were recorded between 300 and 440 nm with an excitation wavelength of 295 nm. The purified and dialyzed samples were incubated with ANS as hydrophobic probe for 5 min at 25 °C. The final concentration of ANS in enzyme solution was 30 μM and the molar ratio of enzyme to ANS was 1:30. The samples were excited at 350 nm and emission spectra were recorded between 380 and 700 nm [37]. Fluorescence results are typical experimental data.

2.2.6. Thermal denaturation measurements

Differential scanning calorimetry (DSC) was performed on Nano-DSC II with two constant cells with a volume of 328 μl. The pressure level of 2 atm was adjusted for preventing bubbles formation. For reversibility measurements, the samples were heated at a rate of 2 °C per min from 10 °C to 80 °C. The scan performance was then done when the sample thermogram passed the T_m (melting point) by 2 °C. The samples were rescanned when they became cold. All samples were normalized by subtracting baseline thermogram using Cpcalc software [38,39]. The melting temperature (T_m) of the luciferase variants was also measured by Cary-Eclipse luminescence spectrophotometer (Varian) with thermostated cell holders where the temperature was kept constant by a circulating water bath. T_m (°C) was calculated from the thermal fluorescence curve. Refolding was followed by monitoring the changes in the intrinsic fluorescence of luciferase variants (after cooling) at 25 °C. The fluorescence emission was recorded between 300 and 400 nm with an excitation wavelength of 295 nm. The unfolding curves were performed by continuous monitoring of changing of Trp intensities over the temperature range of 0–80 °C with a temperature increment of 1 °C/min. All measurements were performed in 50 mM Tris–HCl (pH 7.8) buffer and a protein concentration of 0.02 mg/ml [9].

2.2.7. Molecular dynamics simulation and analysis

The initial coordinates of firefly luciferase were obtained from its crystal structure (PDB ID, 1BA3) [40]. This high-resolution PDB structure has missing residues that their locations were reconstructed using MODELLER v9.15 [41]. The psfgen plugin of VMD 1.9 [42] was used to mutate His461 to Asp and His489 to Asp, Lys or Met. Histidine residues were set to the HSE state, the tautomer protonated on NE2. Similar molecular dynamics (MD) simulations for native and four mutated types of luciferase at 300 and 340 K were performed using NAMD 2.10 [43] package implementing the CHARMM27 [44] force field with CMAP corrections for proteins. Whole systems were solvated using TIP3P water model and ionized to guarantee the electrical neutrality of the system. Systems were subjected to 20000 steps minimization by using the conjugated gradient method. In the equilibration run, first the systems were gradually heated up to 300 and 340 K with a weak restraint on the backbone atoms of the protein and constant Berendsen pressure [45] of 1 bar for 250 ps. Then restraints were gradually removed in 250 ps. The equilibration continued for 1.5 ns with constant temperature at 300 and 340 K. After that, 50 ns production runs were performed without any restraints under NPT conditions using Nosé-Hoover Langevin piston pressure control combined with Langevin dynamics [46,47]. The time step of the equilibration process and production runs set at 1 and 2 fs, respectively. The atom-based cutoff of 12 Å was used to treat both electrostatic and van der Waals interactions. In order to apply smoothing functions, the switch distance cut off of 10 Å was used. The electrostatic interactions were calculated using particle mesh Ewald algorithm (PME) [48] with 1.0 Å grid spacing. The long-range electrostatics and short-range non-bonded interactions were calculated every 2 and 1 fs, respectively. For structural analysis, trajectories were saved every 2 ps. Post-processing analysis of trajectories such as root mean square deviations (RMSDs), root mean square fluctuation (RMSF), intramolecular hydrogen bonds, salt bridges and principal component analysis (PCA) were calculated and analyzed by VMD 1.9 [42] and Mathematica10.4 [49]. Persisting of salt bridges introduced after histidine substitution by aspartate or lysine were identified as ion pairing interactions with more than 10% in the 10 Å vicinity of mutation site. Principal component analysis was used as a tool in exploratory conformational changes. In order to figure out this variance in equilibrium fluctuations, all mutation trajectories were joined together. Then a standard PCA was performed on Cα atoms of the combined trajectory and the covariance matrix were built and diagonalized. Corresponding eigenvectors, directions in conformational space, and eigenvalues, the mean square fluctuations of atoms in the direction of corresponding eigenvectors, were obtained and sorted in decreasing order. The first two principal components correspond to first two highest proportion of variance which are orthogonal. Thus, PCA is used to understand mutational effect across different conformational changes.

3. Results

3.1. MD simulation identifies regions of high mobility in luciferase

Molecular dynamics simulation is a powerful tool to probe fast molecular motions at atomic details [50]. To investigate conformational dynamics of luciferase, 50 ns long MD simulations were performed at two temperatures of 300 and 340 K. The root-mean-square fluctuations (RMSF) of protein backbone atoms were calculated for the firefly luciferase enzyme. RMSF is a measure of average atomic mobility over MD trajectories: the more flexible residues of protein structure show higher RMSF values [50]. As shown in Fig. 1a, the C-terminal domain (residues 440–550) is generally more flexible than the N-terminal domain (residues 1–436). More specifically, residues 199–204, 444–448, 460–463, 475–477, 487–493, 505–509 and 526–529 have higher RMSFs at both temperatures, in line with previous reports [34]. It is notable that the two regions 199–204 and 444–448 are involved in substrate binding [51–54]. Residues 475–477 have exhibited relatively high B-factors, indicating high mobility in crystal structure, and relationship between flexibility of this region and thermal stability has been previously investigated [55]. When RMSF values were mapped on protein structure (PDB ID: 1BA3), it was found that fragments 460–463 and 487–494 with high RMSF values are located in surface loops (Fig. 1b). These two fragments contain histidine residues: His461 is located in the loop between helix 13 and β-turn E1 and His489 is placed in the loop between β-turn E2 and helix 14.

3.2. Rational design of histidine-substituted luciferase mutants

As mentioned above, the lower content of histidine and higher

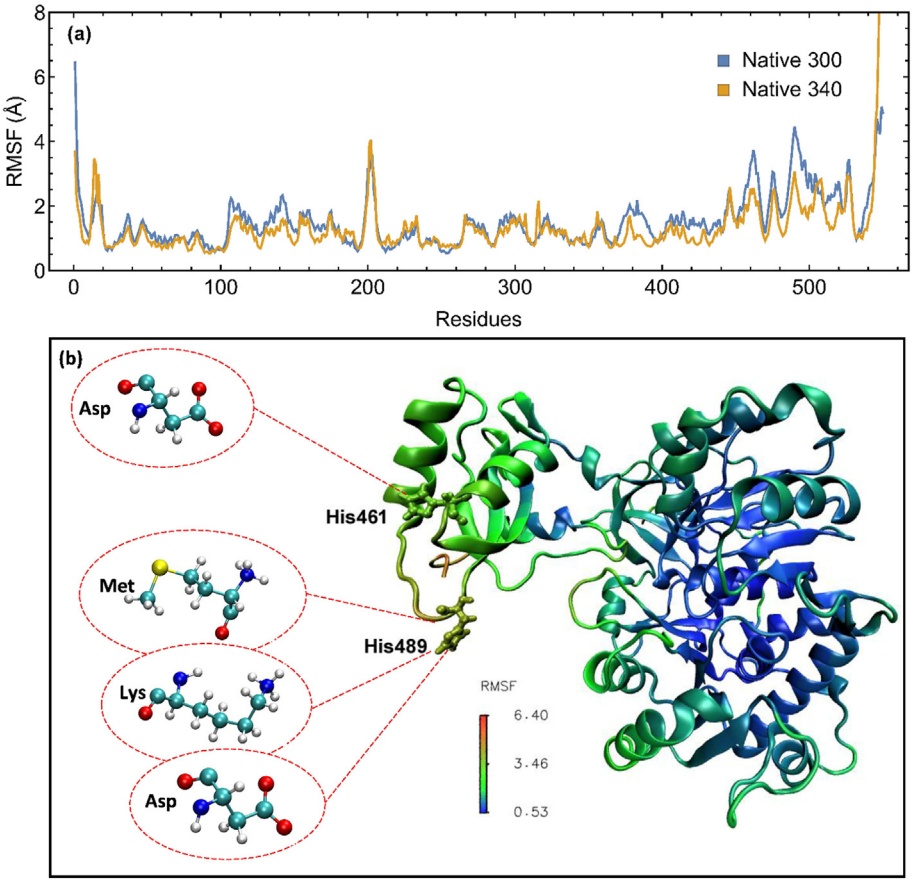

Fig. 1. (a) RMSF evaluation of *P. pyralis* firefly luciferase in 50 ns MD simulation at 300 and 340 K. (b) Schematic representation of *P. pyralis* luciferase colored by variable RMSF value from blue (low RMSF) to red (high RMSF). Two Histidine residues at the position 461 and 489 are shown in the C-terminal domain of *P. pyralis* luciferase. In the present work, His 461 is substituted by Asp and H489 is substituted by Met, Lys and Asp. (For interpretation of the references to colour in this figure legend, the reader is referred to the web version of this article.)

content of charged residues are associated with the enhanced thermostability of proteins. In order to substitute the appropriate residues for mutation sites, Eris web server (protein stability prediction and design) is used. Eris calculates the change of the protein stability induced by mutations (ΔΔG), utilizing the recently developed Medusa modeling suite [56,57]. Eris results demonstrated that substitution of histidine by aspartate at position 489 enhance protein stability of luciferase more than glutamate substitution. However, substitution of His489 by lysine and arginine reduce the luciferase stability. The stability of luciferase decreased more by lysine in comparison with arginine. Eris web server results show that substitution of H461 by aspartate is more appropriate than other amino acids. We therefore decided to replace histidine residues located in flexible loops (His461 and His489) by aspartate in order to enable salt bridge formation and new hydrogen bond interactions. We expected that the additional interactions for H461D and H489D rigidify protein structure and enhance its thermal stability in comparison with the destabilized luciferase structure that is predicted for H489K. In addition, we prepared His489 to methionine mutant in order to figure out the particular importance of histidine side chain interactions, as otherwise methionine and histidine due to similar size and mass (149 and 155 Da, respectively) impose similar steric restrictions.

3.3. Salt bridge formation in histidine-substituted mutants

The ion pairing interactions between negatively-charged side chains of aspartate or glutamate and positively-charged side chains of lysine or arginine contribute to the stability of protein structures [31]. To investigate how histidine substitution by aspartate or lysine influenced ion pairing interaction, we searched for persisting salt bridges introduced in the vicinity of mutation sites. Table 1 shows the number of salt bridges for each luciferase mutant. Surprisingly, H461D mutation decreased the number of neighboring salt bridges from five in the native protein to four, the Glu497-Lys491 salt bridge was no longer stable in the mutated protein (Table 1). Contrary to H461D mutation, the H489D mutation significantly increased the number of neighboring salt bridges from one in the native protein (at 300 K) to five: Asp489 tended to pair with Arg112 and Lys491while its proximal residue Glu488 was capable of pairing with Arg112. The alternate pairing of Glu488 and Asp489 with Arg112 makes a remarkably stable contact between the N- and C-terminal domains of the H489D mutant: the average distance between the two domains decreases to 3.60 Å (Fig. 2). Notably, the added salt bridges are largely temperature-labile and lost at the elevated temperature of 340 K. A similar increase in the number of salt bridges is found in the H489K mutant, where in contrast with the H489D mutant, the introduced salt bridges are largely temperature-stable. Despite the inability of methionine side-chain itself in making salt bridges, the H489M mutation could similarly increase the number of salt bridges, even though the particular identity of salt bridges were different from H489D or H489K mutant (Table 1). The effect of newly introduced salt bridges on luciferase flexibility will be addressed in a following section.

Table 1
The most possibility of salt bridge interactions between residues during the 50 ns simulation.

	300 K		340 K	
Native (His461)	ASP500-LYS496 GLU488-LYS491 GLU497-LYS496	GLU495-LYS496 GLU497-LYS491	ASP500-LYS496 GLU488-LYS491 GLU497-LYS496	GLU495-LYS496 GLU497-LYS491
H461D	ASP500-LYS496 GLU488-LYS491	GLU495-LYS496 GLU497-LYS496	ASP500-LYS496 GLU488-LYS491	GLU495-LYS496 GLU497-LYS496
H489K	ASP520-LYS489 ASP520-LYS549	GLU488-LYS489 GLU488-LYS491	ASP520-LYS489 ASP520-LYS549 GLU113-ARG112	GLU488-LYS489 GLU488-LYS491
H489D	ASP489-ARG112 ASP489-LYS491 ASP520-LYS549	GLU488-ARG112 GLU488-LYS491	ASP489-ARG112	GLU488-LYS491
H489M	GLU495-LYS547 GLU495-LYS549 GLU497-LYS491	GLU497-LYS496 GLU521-LYS524	ASP466-LYS524 GLU113-ARG112	GLU488-LYS491 GLU521-LYS524
Native (His489)	GLU488-LYS491		ASP520-LYS549	GLU488-LYS491

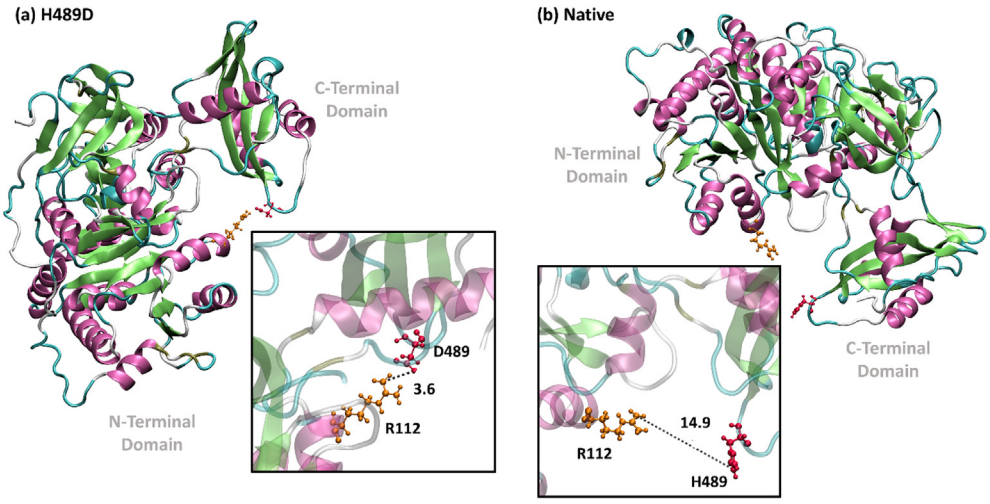

Fig. 2. 3D structure of native and mutant of luciferase (H489D). Substitution of His489 by ASP modifies the conformation of firefly luciferase. By the new conformation, stable contact is observed between Arg112 at the N-terminal and Asp489 at the C-terminal domains. (a) The shorter distance (3.60 Å) is observed for H489D, between aspartate (red color) and arginine (yellow color). (b) For native form, the distance between Arg and Asp is 14.99 Å. (For interpretation of the references to colour in this figure legend, the reader is referred to the web version of this article.)

3.4. Hydrogen bond formation in histidine-substituted mutants

Like salt bridges, intramolecular hydrogen bonds play significant roles in thermostability of proteins [58]. To address whether histidine mutation alters the hydrogen bond networks surrounding the mutation site, hydrogen bonds were measured in 6 Å proximity of residues 461 and 489 (Table 2). The results show that in the vicinity of His461 in native luciferase, residues His461, Tyr501, Val502 and Gln505 participated in the formation of hydrogen bonds at 300 K. After H461D mutations, the total number of neighboring hydrogen bonds decreased, while the number of hydrogen bonds involving residue 461 itself increased from three in the native protein to six. A particularly high hydrogen bond propensity was observed between Asp461 and Asn463 in the mutated protein. The hydrogen bonds between Asp461 and Asn463 were temperature-stable and preserved at the elevated temperature of 340 K. At position 489, hydrogen bonds occurred between Glu488 and Lys491, and between Phe465 and Val486. Upon H489D mutation, the hydrogen bond between Phe465 and Val486 was disrupted, while more hydrogen bond modes were detected between Glu488 and Lys491. Similarly, in the H489K mutant, Glu488 showed promiscuous hydrogen bonding tendency: it could interact not only with Lys491 but also Asn463 and Lys489. Similar changes were observed after H489M mutation.

3.5. Conformational dynamics of luciferase are variably affected by histidine substitution

Thus far, we have demonstrated that histidine substitution leads to significant alterations in salt bridges and hydrogen bonds around mutation sites. The next step is to evaluate how the altered interactions affect protein conformational dynamics. To address this question, the RMSF of Cα atoms were calculated at 300 K and compared among various luciferase mutants (Fig. 3). Overall, H461D, H489K and native luciferase were more flexible than H489M and H489D. Despite high general mobility, the H461D mutant showed restricted mobility at residues 455–470, which is probably due to the local strengthening of hydrogen bond network after mutation (see above).

Further support for the higher flexibility of H461D mutant at low temperature is provided by the root-mean-square deviation (RMSD) of protein backbone atoms when compared with the starting structure. As shown in Fig. 4a, the H489D, H489M and native luciferase are very stable throughout the simulation time at

Table 2
The most possibility of hydrogen bond interactions between residues during the 50 ns simulation.

	300 K		340 K	
Native (His461)	ASN463 … HIS461	GLN505 … TYR501	ASN463 … HIS461	HIS461 … LEU458
	VAL502 … ILE498	GLN505 … TYR501	TYR501 … GLU497	ILE464 … HIS461
	TYR501 … GLU497	ILE464 … HIS461	TYR501 … ILE457	
	TYR501 … ILE457	GLN460 … SER456		
	GLN505 … VAL502	GLN460 … TYR501		
	HIS461 … LEU458	GLN460 … SER456		
H461D	TYR501 … ILE457	ASP 461 … LEU458	TYR501 … ILE457	ILE464 … ASP461
	ASN463 … ASP461(4)[a]	ILE464 … ASP461	ASN463 … ASP461(4)	ASP461 … LEU458
			GLN505 … TYR501	GLN505 … TYR501
H489K	GLU488 … ASN463	LYS489 … GLU488(2)[a]	PHE465 … VAL486	LYS491 … GLU488(3)[a]
	LYS491 … GLU488			
H489D	LYS491 … GLU488 (3)[a]		LYS491 … GLU488(7)[a]	
H489M	VAL519 … VAL485	ASN463 … GLU488 (2)[a]	GLU488 … ASN463	LYS491 … GLU488 (5)[a]
	GLU488 … ASN 463		PHE 465 … VAL486	
Native (His489)	PHE465 … VAL486	LYS49 … GLU488	LYS491 … GLU488(4)[a]	

[a] The number of interactions.

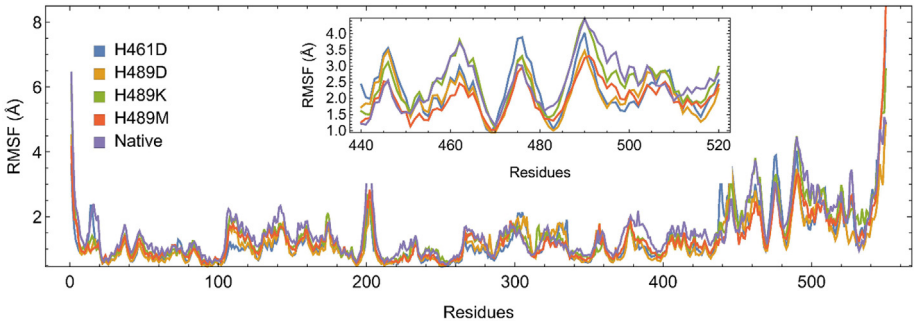

Fig. 3. Comparison of RMSF values of native and mutants of firefly luciferase in 50 ns MD simulation at 300 K. The inset represents the fluctuation of C-terminal domain residues of native and mutations.

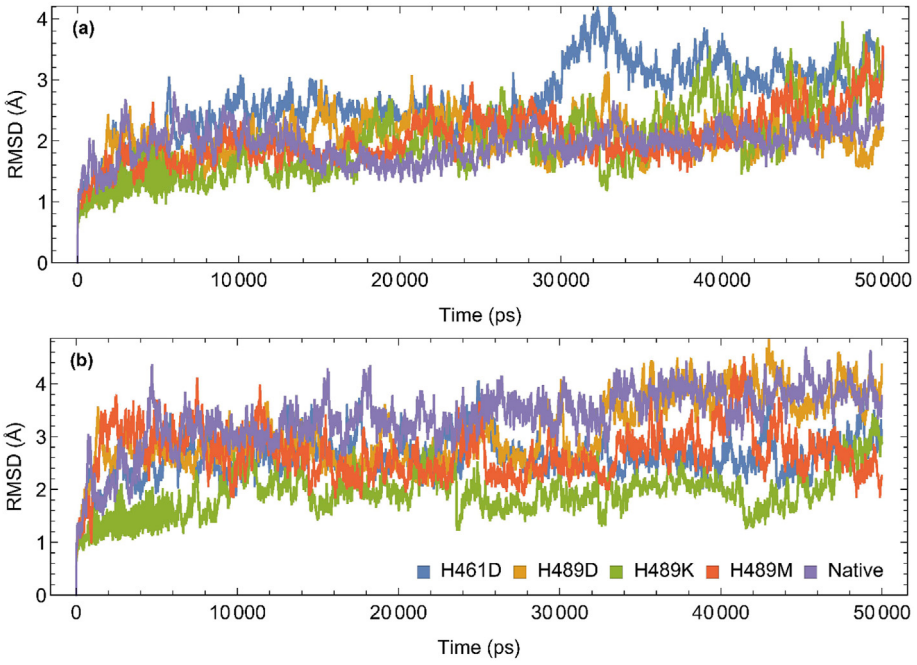

Fig. 4. Root mean squared deviation (RMSD) of Cα atoms as a function of time were calculated in 50 ns of molecular dynamics simulation at two temperatures of (a) 300 K and (b) 340 K.

300 K, while the H489K and especially H461D mutants appear to more extensively sample the conformational space. The H461D mutant exhibits a sharp rise in RMSD after 30000 ps, which is likely to denote a structural transition. It is noteworthy that the distinct flexibility of H461D form is not observed at 340 K (Fig. 4b).

To better understand collective motions in luciferase in dependence of histidine mutation, we performed principal component analysis (PCA) of the MD trajectories. Through this analysis, the conformational mobility of proteins over the MD trajectories is captured in a remarkably small number of principal components. As a result, instead of following protein structures in high-dimensional conformational spaces, one can monitor protein mobility in much lower dimensional sub-spaces. Fig. 5a presents the relative cumulative variance of the first 30 eigenvectors of all mutations joined trajectory at 300 and 340 K. The first five eigenvectors of the PCA analysis at 300 K had larger eigenvalues than 340 K, which shows trajectories experienced a larger fluctuation during simulation at 300 K. Fig. 5b and c shows the MD ensembles of our five luciferase variants at 300 and 340 K, respectively, as projected on the first two principal components (PC1 and PC2). There, each point represents a distinct conformational sub-space occupied by the protein at a certain time during MD simulation. Interestingly, at 300 K, the essential sub-space explored by the H461D mutant was remarkably distinct from the other four mutants, which occupied overlapping regions. At 340 K, however, a high level of overlap was observed among all five mutants.

3.6. Enzyme kinetic and stability properties

To evaluate the effect of mutations on the enzymatic activity of luciferase, various activity parameters were determined (Table 3). First, bioluminescence emission spectra of the mutated enzymes did not show any significant shift of the peak when compared to the native enzyme. Since emission spectral features of luciferase are determined by solvent accessibility of luciferin binding site [59], the lack of significant spectral changes indicate that solvent access to the binding site has not been altered upon mutation.

Second, we determined binding affinities for the two substrates ATP and luciferin (LH_2) separately through Lineweaver-Burk plots. As indicated in Table 3, the obtained K_m values for ATP followed the order H461D > H489D > H489K ~ native > H489M. On the other hand, the K_m for LH_2 followed the order H461D ~ native > H489D > H489M > H489K.

Then, the enzyme activity profile in dependence of pH and temperature was determined. Relative specific activity of the H461D mutant was around 40% of the native form, while other mutations exhibited specific activities similar to the native form. The optimum pH was not affected by His461 or His489 mutations (pH 8.5), but the optimum temperature exhibited intriguing shifts (Table 3): the H489K mutant showed a 5 °C increase in the optimum temperature, that of H489D remained the same, and those of H489M and particularly H461D decreased. The optimum temperature of H461D enzyme was 10 °C, indicating cold adapted behavior in this mutated enzyme. We also studied the rate of thermal denaturation and inactivation in different luciferase mutants. After incubation at various temperatures for various times, remaining enzyme activity was quantified as the percent of the original activity (Fig. 6a, b, 6c and 6d). In line with the observed changes in the optimum temperature, the thermal inactivation rate of H461D was higher than the native enzyme, while H489D had a slightly smaller inactivation rate (Fig. 6d).

3.7. Structural properties

To probe tertiary structural changes in luciferase after histidine substitution, we performed intrinsic tryptophan and extrinsic ANS fluorescence experiments. Tryptophan fluorescence is highly sensitive to the environment polarity and ANS, a hydrophobic dye non-fluorescent in aqueous solutions, becomes fluorescent when it binds to hydrophobic patches of proteins [55]. *P. pyralis* luciferase contains two Trp residues, Trp417 and Trp426, both of which are situated in the distal region of the N-terminal domain close to the hinge region [36,60]. They are not surface residues, although Trp426 is near the protein surface [37]. MD simulation data demonstrate that flexibility of Trp residues are altered by histidine substitution: average RMSF of the two Trp residues are 1.6, 1.4, 1.1 and 0.9 Å for the H489D, H461D, H489M and H489K mutants, respectively, compared to ~0.8 Å for the native form. As shown in Fig. 7a, Trp fluorescence intensity increased in H489D and H489M mutants when compared with the native form. Conversely, the H489K and H461D mutants exhibited a decrease in Trp fluorescence intensity. Regarding ANS fluorescence, histidine substitutions led to intensity changes at various levels (Fig. 7b). Together, our Trp and ANS fluorescence data suggest that the tertiary structure of luciferase is altered by histidine mutations, in terms of local environment of its tryptophans and general hydrophobicity of its exposed surface.

3.8. Thermodynamic stability

Thermophilic enzymes are stable, but poorly active at low temperatures. In contrast, most cold-adapted enzymes found in

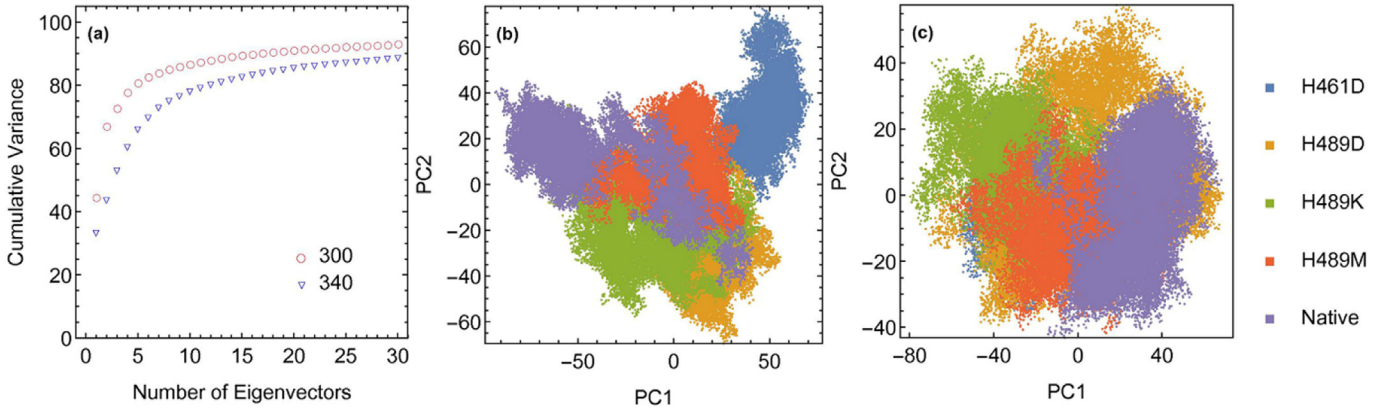

Fig. 5. (a) Relative cumulative variance of the first 30 eigenvectors and the conformational sampling of different mutations of luciferase as a function of the first two principal components PC1 and PC2 obtained from the PCA analysis on the Cα atoms coordinate of the mutations at (b) 300 K and (c) 340 K.

Table 3
Kinetic properties of the native and mutants of luciferase.

	K_m		Relative Specific Activity (%)	λ_{max} (nm) at pH 7.8	Optimum Temperature (°C)	Optimum pH
	LH_2 (μm)	ATP (μm)				
Native	5 ± 0.3	60 ± 3	100 ± 5	560	25	8.5
H461D	5 ± 0.2	100 ± 5	57.6 ± 2.9	560	10	8.5
H489K	2 ± 0.1	60 ± 4	115 ± 6	560	30	8.5
H489D	2.5 ± 0.2	90 ± 5	112 ± 6	560	25	8.5
H489M	2.3 ± 0.1	40 ± 3	103 ± 5	560	20	8.5

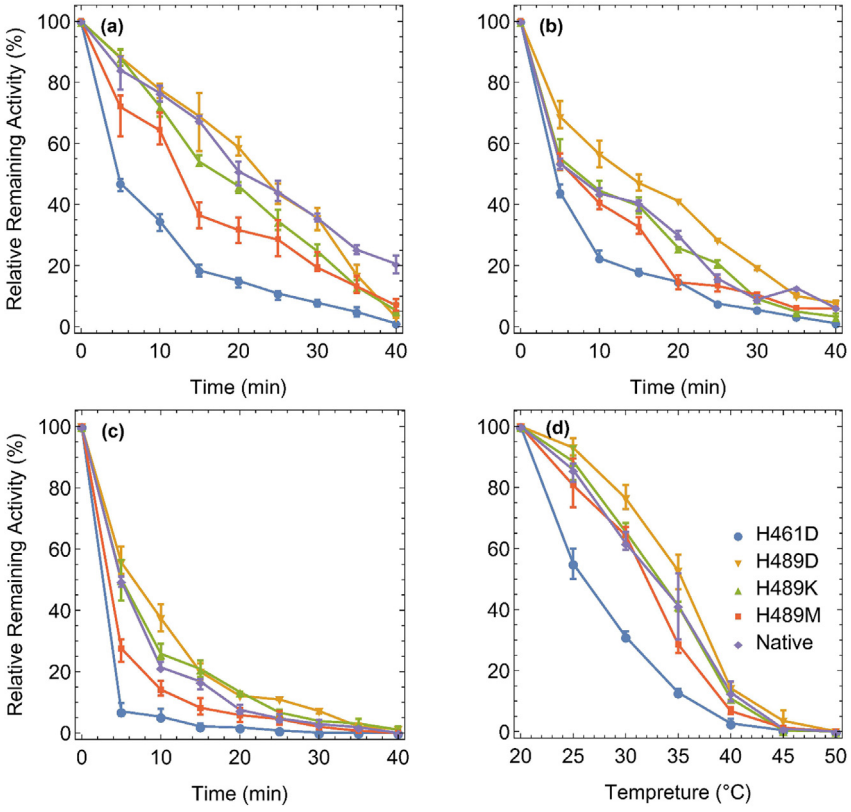

Fig. 6. Thermal stability curves of native and mutant firefly luciferases were determined from 0 to 45 min and these data are shown as the percentage of the original activity at the temperatures of (a) 25 °C (b) 30 °C and (c) 35 °C. (d) Thermal inactivation curve of native and mutants, luciferase remaining activities were determined at 20–50 °C and shown as the percentage of the original activity.

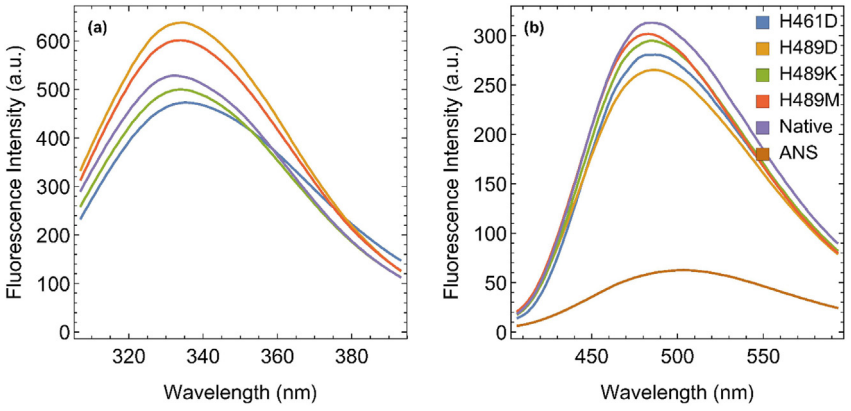

Fig. 7. (a) Intrinsic fluorescence spectra for native and mutant forms of firefly luciferase. (b) Fluorescence spectra of ANS in the presence of native and mutant luciferases.

nature are less stable but substantially more active at low temperatures [61,62]. Various kinds of non-covalent interactions raise the transition-state energy barrier for denaturation. Thermostable enzymes are generated by amino acid substitution to increase structural rigidity, restrict conformational flexibility and increase interactions between unstable domains [28]. The melting temperature (T_m) is a representative parameter for protein thermostability. Assuming two-state protein folding, T_m is defined as the temperature at which both the folded and unfolded states are equally populated at equilibrium. In other words, T_m is the temperature that the standard Gibbs free energy (ΔG°) of the thermal unfolding process is zero [63]. In order to gain deeper insights into the stability of mutated enzymes, thermal denaturation midpoints (T_m) were determined by DSC and intrinsic fluorescence experiments (Table 4). In DSC the temperature scans from 10 to 85 °C clearly showed a single peak, therefore thermal unfolding can be well approximated by a two-state transition model. T_m for native form (40.8 °C) is similar to the previously reported value [38,39]. T_m for various luciferase mutant followed the order H489D > native ~ H489K > H489M > H461D. The melting point of H461D luciferase was 26.2 °C, meaning that, in equilibrium, half of the protein is unfolded at this temperature.

Thermal denaturation of luciferase was further studied by protein intrinsic fluorescence. The two Trp residues of *P. pyralis* luciferase, Trp417 and Trp426, are relatively buried in the folded-state of protein [37], but after thermal unfolding and potential increase in their solvent exposure, their fluorescence behavior is altered. Following temperature dependence of protein fluorescence spectra, the melting point of the structural conformation could be obtained, which were approximately similar to those of DSC data (Table 4). We also estimated standard Gibbs free energy (ΔG°) of thermal unfolding from the Pace analysis [64]. The estimated ΔG°_{298}, Gibbs free energy of protein denaturation at 25 °C for native and mutants, followed the order H489D > native > H489K ~ H489M > H461D. The slightly higher conformational stability of H489D could be caused by the increased number of salt bridges. The H461D had the lowest T_m and ΔG°_{298}, which is further discussed below.

4. Discussion

Increasing hydrogen bond interactions of Asp residue at position 461 (H461D) in the thermal sensitive region 460–463 rigidifies local structure of firefly luciferase, while global flexibility is increased. These new hydrogen bond interactions are conserved at the elevated temperature. Kinetic parameters showed that the H461D variant is deactivated more quickly at 35 °C, and the optimum temperature of this new enzyme is shifted down to below 15 °C. Melting temperature and ΔG° of denaturation of H461D are rather low when compared with the other mutations (26.2 °C and 9.4 ± 2 kJ/mol). The MD data demonstrates that the salt bridge Glu497-Lys491 is lost in the H461D mutant, a finding which suggests that this salt bridge may play a particularly important role in thermal stability of luciferase. Together, based on the higher flexibility and lower thermal stability of this mutant, we conclude that the H461D mutation has induced a behavior typical of cold adapted enzymes in luciferase like Tibetan firefly luciferase [65].

Psychrophilic organisms thrive in cold environments through cold-adapted proteins with peculiar structural and dynamical features. The key element in cold adaptation is high conformational flexibility, especially around the active site, which enables protein activities even at very low temperatures [66]. The high conformational flexibility is generally achieved by protein sequence evolution along with a reduction in the number of salt bridges and hydrogen bonds and in the degree of compaction of protein hydrophobic cores. The advantage of higher activity at cold temperature however comes at the cost of low substrate binding affinity and thermal instability [67,68] In line with the common features of psychrophilic enzymes, the H461D luciferase showed a 15 °C drop in its optimum temperature compared to the native enzyme (from 25 to 10 °C, Table 3), had lowest binding affinities (highest K_m values) for ATP (Table 3) and poor thermal stability both in functional and structural terms (Figs. 6, 7 and Table 4). Importantly, our MD simulation data suggests that the psychrophilic behavior of H461D mutant could be originated by the higher flexibility of its functional regions at low temperatures, as evidenced by its high RMSF and RMSD values at 300 K (Figs. 3 and 4) and suggested by its altered collective motions (Fig. 5). The higher flexibility of the H461D mutant is probably caused by a decrease in the number of salt bridges and hydrogen bonds (Tables 1 and 2).

Methionine in H489M mutant changes the platform of hydrogen bond and salt bridge interactions in the region 487–494. T_m value of H489M is 36.6 °C and H489M thermal inactivation curve shows that H489M loses 75% of its activity at 35 °C. Presumably, the lower stability of H489M compared to native is related to the salt bridge 488–491, which is lost in the H489M mutant as shown by MD data. While half-life and ΔG°_{298} for H489K and H489M are approximately similar, kinetics stability and melting temperature are clearly different (Table 3 and Fig. 6). T_m value of H489K and native are similar, 40.6 and 40.8; respectively. Thermal inactivation curve displays native and H489K preserve 41% of the original activity while H489D preserves 52% of the original activity at 35 °C. Half-life of H489K is similar to H489D and native form at 35 °C, while at 25 °C, H489K has lower stability. The optimum temperature for H489K increase 5 °C than native and H489D. Lysine in H489K mutant participates in two salt bridges and hydrogen bond interactions but these new interactions cannot change the thermal stability of the H489K mutant. Substitution of His489 by Lys slightly alter the function and structure of native luciferase.

MD simulation data indicate a rigid conformation in the H489D mutant. A higher number of salt bridges were observed in this mutant. Particularly, the two salt bridges Asp489-Arg112 and Glu488-Arg112 seem to be crucial for the rigidity of tertiary structure in H489D. As expected, Asp489 participates in salt bridge and hydrogen bond interactions thereby increases the $t_{1/2}$ and kinetics stability of luciferase at 25 and 30 °C. Despite its rigid structure, the H489D mutant cannot preserve their active structures at high temperatures.

Histidine 461and His489 are exposed at the surface of their loops and interact with their nearby residues. However, the number of salt bridges and hydrogen bond interactions for His489 is relatively low. In H489K mutant, the flexible side chain of lysine being located at the surface of the loop fails to provide additional interactions required for an improved thermal stability. In

Table 4
Half-lives and structural properties of native and mutants of luciferase.

	[a] $t_{1/2}$ (min)			[b] ΔG°_{298} (kJ/mol)	[c] T_m (°C)	
	25 °C	30 °C	35 °C		[d]DSC	[e]FLU
Native	17.4 ± 1	10.5 ± 1	6.1 ± 1	16.7 ± 2	40.8	40.3 ± 0.2
H461D	9.5 ± 1	6.9 ± 1	3.7 ± 1	9.4 ± 2	26.2	32.9 ± 0.6
H489K	12.6 ± 1	8.3 ± 1	6.4 ± 1	15.5 ± 2	40.6	40 ± 0.7
H489D	20.2 ± 1	11.1 ± 1	6.5 ± 1	17.9 ± 2	42	40.6 ± 0.5
H489M	12.4 ± 1	9.5 ± 1	5.7 ± 1	15.6 ± 2	36.6	39 ± 0.8

[a] Half-life.
[b] Gibbs free energy of denaturation.
[c] Melting temperature.
[d] Melting temperature from differential scanning calorimetry experiment.
[e] Melting temperature from fluorescence intensity experiment.

comparison, the side chain of aspartate is smaller and less flexible, enabling more interactions in the 487–494 region of the H489D mutant. However, the increased number of local interactions in the H489D mutant does not lead to a significant improvement in its thermal stability. Unlike H489, substitution of H461 by aspartate significantly reduces protein thermal stability. Our results suggest that substitution in His461 is probably has more effect in thermal stability of luciferase than H489.

5. Conclusion

Firefly luciferase is a light emitting enzyme with widespread use in clinical and industrial applications. Our data demonstrate that the MD simulation can be used to design enzyme mutants with altered conformational dynamics and thermal stability. Enhancement the number of salt bridges and hydrogen bonds are believed to increase protein thermal stability. However, our results represent that increasing the number of salt bridges and hydrogen bonds can improve thermostability of H489D and H489K slightly. Moreover, by increasing the number of hydrogen bonds for H461D, this mutation behaves as a psychrophilic enzyme. So, rather than fundamental aspect of this change, this psychrophilic luciferase can be potentially utilized in the particular low working temperatures in industrial and medical applications.

Acknowledgments

The authors are thankful to Ms. Faezeh Moosavi-movahedi, Ms. Atiyeh Ghasemi and Ms. Najmeh Poursasan for providing the necessary facilities for the preparation of this paper. The financial support of Research Council of University of Tehran is highly appreciated.

References

[1] H. Fujii, K. Noda, Y. Asami, A. Kurod, M. Sakata, M. Tokida, Increase in bioluminescence intensity of firefly luciferase using genetic modification, Anal. Biochem. 366 (2007) 131–136.
[2] A. Riahi-Madvar, S. Hosseinkhani, Design and characterization of novel trypsin resistant firefly luciferases by site-directed mutagenesis, Protein Eng. Des. Sel. 22 (11) (2009) 655–663.
[3] E. Conti, N.P. Franks, P. Brick, Crystal structure of firefly luciferase throws light on a superfamily of adenylate-forming enzymes, Structure 4 (3) (1996) 287–298.
[4] M. Kheirabadi, Z. Sharafian, H. Naderi-Manesha, U. Heineman, U. Gohlke, S. Hosseinkhani, Crystal structure of native and a mutant of *Lampyris turkestanicus* luciferase implicate in bioluminescence color shift, Biochim. Biophys. Acta 1834 (12) (2013) 2729–2735.
[5] B.S. Alipour, S. Hosseinkhani, S.K. Ardestani, A. Moradi, The effective role of positive charge saturation in bioluminescence color and thermostability of firefly luciferase, Photochem. Photobiol. Sci. 8 (2009) 847–855.
[6] B.R. Branchini, T.L. Southworth, N.F. Khattak, E. Michelini, A. Roda, Red and green-emitting firefly luciferase mutants of bioluminescent reporter applications, Anal. Biochem. 345 (2005) 140–148.
[7] P.I. Zhuravlev, C.K. Materese, G.A. Papoian, Deconstructing the native state: energy landscapes, function, and dynamics of globular proteins, J. Phys. Chem. B 113 (2009) 8800–8812.
[8] Y. Wang, Y. Hayamizu, H. Akiyama, Spectroscopic study of firefly oxyluciferin in an enzymatic environment on the basis of stability monitoring, J. Phys. Chem. B 118 (2014) 2070–2076.
[9] A. Riahi-Madvar, S. Hosseinkhani, F. Rezaee, Implication of Arg213 and Arg337 on the kinetic and structural stability of firefly luciferase, Int. J. Biol. Macromol. 52 (2013) 157–163.
[10] P. White, D. Squirrell, P. Arnaud, C. Lowe, J. Murray, Improved thermostability of the North American firefly luciferase: saturation mutagenesis at position 354, Biochem. J. 319 (2) (1996) 343–350.
[11] B.R. Branchini, D.M. Ablamsky, A.L. Davis, T.L. Southworth, B. Butler, F. Fan, A.P. Jathoul, M.A. Pule, Red-emitting luciferases for bioluminescence reporter and imaging applications, Anal. Biochem. 396 (2010) 290–297.
[12] M.I. Koksharov, N.N. Ugarova, Thermostabilization of firefly luciferase by in vivo directed evolution, Protein Eng. Des. Sel. 24 (11) (2011) 835–844.
[13] R.M. Bannen1, V.S. Suresh, G.N. Phillips Jr., J. Stephen, S.J. Wright, J.C. Mitchell, Optimal design of thermally stable proteins, Bioinformatics 24 (20) (2008) 2339–2343.
[14] B.M. Nestl, B. Hauer, Engineering of flexible loops in enzymes, ACS Catal. 4 (2014) 3201–3211.
[15] Z.S. Hendsch, T. Jonsson, R.T. Sauer, B. Tidor, Protein stabilization by removal of unsatisfied polar groups: computational approaches and experimental tests, Biochemistry 35 (24) (1996) 7621–7625.
[16] K. Manjunath, K. Sekar, Molecular dynamics perspective on the protein thermal stability: a case study using SAICAR synthetase, J. Chem. Inf. Model. 53 (9) (2013) 2448–2461.
[17] R. Verma, U. Schwaneberg, D. Roccatano, Computer-aided protein directed evolution: a review of web servers, databases and other computational tools for protein engineering, Comput. Struct. Biotechnol. J. 2 (3) (2012) 1–12.
[18] J. Tian, P. Wang, S. Gao, X. Chu, N. Wu, Y. Fan, Enhanced thermostability of methyl parathion hydrolase from Ochrobactrum sp. M231 by rational engineering of a glycine to proline mutation, FEBS J. 277 (2010) 4901–4908.
[19] M. Nazari, S. Hosseinkhani, Design of disulfide bridge as an alternative mechanism for color shift in firefly luciferase and development of secreted luciferase, Photochem. Photobiol. Sci. 10 (2011) 1203–12115.
[20] K. Steiner, H. Schwab, Recent advances in rational approaches for enzyme engineering, Comput. Struct. Biotechnol. J. 2 (3) (2012) 1–12.
[21] H. Yang, L. Liu, H. Shin, R.R. Chen, J. Li, G. Du, J. Chen, Structure-based engineering of histidine residues in the catalytic domain of α-amylase from Bacillus subtilis for improved protein stability and ccatalytic efficiency under acidic conditions, J. Biotechnol. 164 (2013) 59–66.
[22] S. Chakravarty, R. Varadarajan, Elucidation of factors responsible for enhanced thermal stability of proteins: a structural genomics based study, Biochemistry 41 (2002) 8152–8161.
[23] M. Mortazavi, S. Hosseinkhani, Design of thermostable luciferases through arginine saturation in solvent-exposed loops, Protein Eng. Des. Sel. 24 (12) (2011) 893–903.
[24] M.R. Barnes, I.C. Gray, Bioinformatics for Geneticists, Wiley, 2003.
[25] D.R. Tompa, M.M. Gromiha, K. Saraboji, Contribution of main chain and side chain atoms and their locations to the stability of thermophilic proteins, J. Mol. Graph. Model. 64 (2016) 85–93.
[26] H. Yu, H. Huang, Engineering proteins for thermostability through rigidifying flexible sites, Biotechnol. Adv. 32 (2014) 308–315.
[27] J.C. Joo, S.P. Pack, Y.H. Kim, Y.J. Yoo, Thermostabilization of Bacillus circulans xylanase: computational optimization of unstable residues based on thermal fluctuation analysis, J. Biotechnol. 151 (2011) 56–65.
[28] J. Chen, H. Yu, C. Liu, J. Liu, Z. Shen, Improving stability of nitrile hydratase by bridging the salt-bridges in specific thermal-sensitive region, J. Biotechnol. 164 (2012) 354–362.
[29] B.W. Matthews, Structural and genetic analysis of protein stability, Annu. Rev. Biochem. 62 (1993) 139–160.
[30] C.W. Lee, H.J. Wang, J.K. Hwang, C.P. Tseng, Protein thermal stability enhancement by designing salt bridges: a combined computational and experimental study, PLoS One 9 (11) (2014) 1–12.
[31] S.K. Bharatiy, M. Hazra, M. Paul, S. Mohapatra, D. Samantaray, R.C. Dubey, S. Sanyal, S. Datta, S. Hazra, In silico designing of an industrially sustainable carbonic anhydrase using molecular dynamics simulation, ACS Omega 1 (2016) 1081–1103.
[32] B. Singh, G. Bulusu, A. Mitra, Understanding the thermostability and activity of Bacillus subtilis lipase mutants: insights from molecular dynamics simulations, J. Phys. Chem. B 119 (2) (2015) 392–409.
[33] X.F. Zhang, G.Y. Yang, Y. Zhang, Y. Xie, S.G. Withers, Y. Feng, A general and efficient strategy for generating the stable enzymes, Sci. Rep. 6 (33797) (2016) 1–12.
[34] H. Yu, Y. Zhao, C. Guo, Y. Gan, H. Huang, The role of proline substitutions within flexible regions on thermostability of luciferase, Biochim. Biophys. Acta 1854 (2015) 65–72.
[35] Y. Xie, J. An, G. Yang, G. Wu, Y. Zhang, L. Cui, Y. Feng, Enhanced enzyme kinetic stability by increasing rigidity within the active site, J. Biol. Chem. 289 (11) (2014) 7994–8006.
[36] M. Moradi, S. Hosseinkhani, R. Emamzadeh, Implication of an unfavorable residue (Thr346) in intrinsic flexibility of firefly luciferase, Enzyme Microb. Technol. 51 (2012) 186–192.
[37] A. Moradi, S. Hosseinkhani, H. Naderi-Manesh, M. Sadeghizadeh, B.S. Alipour, Effect of charge distribution in a flexible loop on the bioluminescence color of firefly luciferases, Biochemistry 48 (2009) 575–582.
[38] M. Naderi, A.A. Moosavi-Movahedi, S. Hosseinkhani, M. Nazari, M. Bohlooli, J. Hong, H. Hadi-Alijanvand, N. Sheibani, Implication of disulfide bridge induced thermal reversibility, structural and functional stability for luciferase, Protein Pept. Lett. 22 (1) (2015) 23–30.
[39] P. Maghami, B. Ranjbar, S. Hosseinkhani, A. Ghasemi, A. Moradi, P. Gill, Relationship between stability and bioluminescence color of firefly luciferase, Photochem. Photobiol. Sci. 9 (2010) 376–383.
[40] N.P. Franks, A. Jenkins, E. Conti, W.R. Lieb, P. Brick, Structural basis for the inhibition of firefly luciferase by a general anesthetic, Biophys. J. 75 (1998) 2205–2211.
[41] A. Sali, T. Blundell, Comparative Protein Modelling by Satisfaction of Spatial Restraints. Protein Structure by Distance Analysis, IOS Press, 1994.
[42] W. Humphrey, A. Dalke, K. Schulten, VMD: visual molecular dynamics, J. Mol. Graph. 14 (1) (1996) 33–38.
[43] J.C. Phillips, R. Braun, W. Wang, J. Gumbart, E. Tajkhorshid, E. Villa, C. Chipot, R.D. Skeel, L. Kale, K. Schulten, Scalable molecular dynamics with NAMD, J. Comput. Chem. 26 (16) (2005) 1781–1802.

[44] A.D. MacKerell Jr., D. Bashford, M.L.D.R. Bellott, R.L. Dunbrack Jr., J.D. Evanseck, M.J. Field, S. Fischer, J. Gao, H. Guo, S. Ha, D. Joseph-McCarthy, All-atom empirical potential for molecular modeling and dynamics studies of proteins, J. Phys. Chem. B 102 (18) (1998) 3586–3616.
[45] H.J.C. Berendsen, J.V. Postma, W.F. van Gunsteren, A. DiNola, J.R. Haak, Molecular dynamics with coupling to an external bath, J. Chem. Phys. 81 (8) (1984) 3684–3690.
[46] G.J. Martyna, D.J. Tobias, M.L. Klein, Constant pressure molecular dynamics algorithms, J. Chem. Phys. 101 (5) (1994) 4177–4189.
[47] S.E. Feller, Y. Zhang, R.W. Pastor, B.R. Brooks, Constant pressure molecular dynamics simulation: the Langevin piston method, J. Chem. Phys. 103 (11) (1995) 4613–4621.
[48] U. Essmann, L. Perera, M.L. Berkowitz, T. Darden, H. Lee, L.G. Pedersen, A smooth particle mesh Ewald method, J. Chem. Phys. 103 (19) (1995) 8577–8593.
[49] I. Wolfram Research, Mathematica, Wolfram Research, Inc., Champaign, Illinois, 2016.
[50] S. Vijayakumar, S. Vishveshwara, G. Ravishanker, D.L. Beveridge, Analysis of hydrogen bonding and stability of protein secondary structures in molecular dynamics simulation, (chapter 11) modeling the hydrogen bond, in: Douglas A. Smith (Ed.), ACS Symposium Series, 1994, p. 569.
[51] J.A. Sundlov, D.M. Fontaine, T.L. Southworth, B.R. Branchini, A.M. Gulick, Crystal structure of firefly luciferase in a second catalytic conformation supports a domain alternation mechanism, Biochemistry 51 (2012) 6493–6495.
[52] B.R. Branchini, J.C. Rosenberg, D.M. Fontaine, T.L. Southworth, C.E. Behney, L. Lerna Uzasci, Bioluminescence is produced from a trapped firefly luciferase conformation predicted by the domain alternation mechanism, J. Am. Chem. Soc. 133 (2011) 11088–11091.
[53] B.R. Branchini, T.L. Southworth, M.H. Murtiashaw, S.R. Wilkinson, N.F. Khattak, J.C. Rosenberg, M. Zimmer, Mutagenesis evidence that the partial reactions of firefly bioluminescence are catalyzed by different conformations of the luciferase C-terminal domain, Biochemistry 44 (2005) 1385–1393.
[54] J.P. Waud, G.B. Sala-Newby, S.B. Matthews, A.K. Campbell, Engineering the C-terminus of firefly luciferase as an indicator of covalent modification of proteins, Biochim. Biophys. Acta 1292 (1996) 89–98.
[55] Z. Amini-Bayat, S. Hosseinkhani, R. Jafari, K. Khajeh, Relationship between stability and flexibility in the most flexible region of *Photinus pyralis* luciferase, Biochim. Biophys. Acta 1824 (2012) 350–358.
[56] S. Yin, F. Ding, N.V. Dokholyan, Eris: an automated estimator of protein stability, Nat. Methods 4 (2007), 466–407.
[57] S. Yin, F. Ding, N.V. Dokholyan, Modeling backbone flexibility improves protein stability estimation, Structure 15 (2007) 1567–1576.
[58] M. Paul, M. Hazra, A. Arghya Barman, S. Hazra, Comparative molecular dynamics simulation studies for determining factors contributing to the thermostability of chemotaxis protein "CheY", J. Biomol. Struct. Dyn. 32 (6) (2014) 1–22.
[59] S. Hosseinkhani, Molecular enigma of multicolor bioluminescence of firefly luciferase, Cell. Mol. Life Sci. 68 (2011) 1167–1182.
[60] W.Q. Wang, Q. Xu, Y.F. Shan, G.J. Xu, Probing local conformational changes during equilibrium unfolding of firefly luciferase: fluorescence and circular dichroism studies of single tryptophan mutants, Biochem. Biophys. Res. Commun. 282 (2001) 28–33.
[61] S. Hayashi, S. Akanuma, W. Onuki, C. Tokunaga, A. Yamagishi, Substitutions of coenzyme-binding, nonpolar residues improve the low-temperature activity of thermophilic dehydrogenases, Biochemistry 50 (2011) 8583–8593.
[62] Z.X. Liang, I. Tsigos, T. Lee, V. Bouriotis, K.A. Resing, N.G. Ahn, P. Judith, J.P. Klinma, Evidence for increased local flexibility in psychrophilic alcohol dehydrogenase relative to its thermophilic homologue, Biochemistry 43 (2004) 14676–14683.
[63] T. Zeiske, K.A. Stafford, A.G. Palmer, Thermostability of enzymes from molecular dynamics simulations, J. Chem. Theory Comput. 12 (6) (2016) 2489–2492.
[64] A.A. Saboury, A.A. Moosavi-Movahedi, Derivation of the thermodynamic parameters involved in the elucidation of protein thermal profiles, Biochem. Educ. 23 (3) (1995) 164–167.
[65] Y. Mitani, R. Futahashi, Z. Liu, X. Liang, Y. Ohmiya, Tibetan firefly luciferase with low temperature adaptation, Photochem. Photobiol. 93 (2) (2017) 466–472.
[66] A. Cipolla, F. Delbrassine, J.L. Da Lage, G. Feller, Temperature adaptations in psychrophilic, mesophilic and thermophilic chloride-dependent alpha-amylases, Biochimie 94 (9) (2012) 1943–1950.
[67] K.S. Siddiqui, R. Ricardo Cavicchioli, Cold-adapted enzymes, Annu. Rev. Biochem. 75 (2006) 403–433.
[68] Z.X. Liang, I. Tsigos, T. Lee, V. Bouriotis, K.A. Resing, N.G. Ahn, J.P. Klinman, Evidence for increased local flexibility in psychrophilic alcohol dehydrogenase relative to its thermophilic homologue, Biochemistry 43 (46) (2004) 14676–14683.